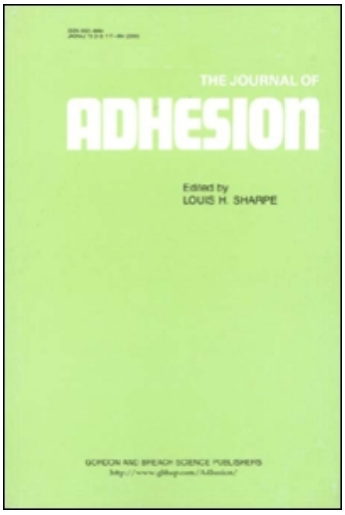

The Journal of Adhesion

Publication details, including instructions for authors and subscription information:
http://www.informaworld.com/smpp/title~content=t713453635

Mode-l Fracture Behaviour of Adhesive Joints. Part II. Stress Analysis and Constraint Parameters

Hamid Reza Daghyani[a]; Lin Ye[a]; Yiu-Wing Mai[a]
[a] Centre for Advanced Materials Technology, Department of Mechanical and Mechatronic Engineering, The University of Sydney, Sydney, Australia

To cite this Article Daghyani, Hamid Reza , Ye, Lin and Mai, Yiu-Wing(1995) 'Mode-l Fracture Behaviour of Adhesive Joints. Part II. Stress Analysis and Constraint Parameters', The Journal of Adhesion, 53: 3, 163 — 172
To link to this Article: DOI: 10.1080/00218469508009936
URL: http://dx.doi.org/10.1080/00218469508009936

J. Adhesion, 1995, Vol. 53, pp. 163–172
Reprints available directly from the publisher
Photocopying permitted by license only

Mode-I Fracture Behaviour of Adhesive Joints. Part II. Stress Analysis and Constraint Parameters

HAMID REZA DAGHYANI, LIN YE* and YIU-WING MAI

Centre for Advanced Materials Technology, Department of Mechanical and Mechatronic Engineering, The University of Sydney, Sydney, NSW 2006, Australia

(Received July 4, 1994; in final form February 16, 1995)

The constraint effect on the fracture behaviour of a rubber-modified epoxy was investigated using compact tension (CT) adhesive joints. An elastic-plastic finite element analysis was conducted to evaluate the stress distribution ahead of the crack tip in the bulk adhesive and adhesive joints of different bond thickness. The models with sharp and finite radius crack tips were evaluated in the analyses. The constraint effect of adherends on the stress triaxiality ahead of the crack tip in the adhesive joints were discussed. The constraint parameters were investigated using the *J-Q* theory and the *J*-CTOD relationship. It was found that as the adhesive thickness was increased, the stress triaxiality ahead of the crack tip was relieved by the remarkable deformation of the adhesive material. Similarly, the crack tip constraint was reduced with increasing bond thickness so that the fracture energy increased towards the value of the bulk adhesive. A higher constraint was associated with a lower fracture energy and *vice versa*. Furthermore, the J-integral did not have a unique relationship with the crack-tip opening displacement (CTOD) for different adhesive bond thickness, as this depends on the constraint around the crack tip. The results of this study will help improve reliability assessment of adhesive joints in engineering applications.

KEY WORDS adhesive joints; bond thickness; fracture energy; constraint; finite element analysis; J-Q theory; crack opening displacement.

1 INTRODUCTION

Crack propagation in adhesive joints is of great importance for reliability assessment in many advanced structural adhesives such as those used in aircraft constructions. Some attempts have been made to investigate the fracture behaviour of adhesive joints using test specimens such as the double-cantilever-beams (DCB)[1–3] and compact tension (CT)[4] geometries. One objective of these studies was to evaluate the effect of bond thickness on the fracture energy of adhesive joints. However, no simple relationship between the crack growth resistance and the bond thickness was found. The reasons for the variation of the fracture energy with bond thickness were mainly attributed to the change in the size of the plastic zone formed around the crack tip and/or fracture surface morphology of the adhesive.[1–3] In fact, the constraint imposed by the adherends influences both the crack tip stress and strain fields and it also controls the

* Corresponding author.

plastic zone size and shape. Several investigations have been carried out to simulate the stress state at the crack tip.[5–8] These analyses were conducted using both two-and three-dimensional finite element models but the mechanical behaviour of adhesive materials was mostly considered to be elastic. Also, in previous analyses for the DCB adhesive joints[5,9] a sharp crack tip with singular finite elements was used which resulted in a singular stress state. Therefore, to investigate thoroughly the effects of nonlinear behaviour of the adhesives, the formation of the plastic zone and the fracture energy of the adhesive joints as well as their interactions with the constraint of adherends, a comprehensive elastic-plastic analysis is required.

In Part I of this paper,[10] CT adhesive joints with a rubber-modified epoxy were used to obtain the relationship between the fracture loads and bond thickness. Then, the fracture energy represented by the critical J-integral, J_c, was evaluated using elastic-plastic finite element analysis (FEA). The constraint effect of adherends on the deformation mechanisms of the adhesive material was discussed using scanning electron microscopy (SEM). In Part II here, the constraint effect of adherends on stress distribution, stress triaxiality as well as the relationship between J and crack-tip opening displacement (CTOD) are investigated using large strain elastic-plastic finite element models.

2 FINITE ELEMENT MODELLING

Based on the compact tension (CT) adhesive joint, finite element models (FEM) were generated. Because of symmetry, only the upper half of the CT specimen was used (Fig. 1a). Some typical properties of the adhesive are:[11] Young's modulus (E) = 3.15 GPa, ultimate strength (σ_u) = 81 MPa and Poisson's ratio (ν) = 0.35. Similar properties for the 6061 aluminium alloy are: $E = 71$ GPa, $\sigma_u = 126$ MPa and $\nu = 0.30$. All finite element analyses (FEA) were carried out assuming linear-elastic behaviour for the adherends and elastic-plastic behaviour for the adhesive material. The nonlinearity of the adhesive material was described by the uniaxial stress-strain curve determined according to ASTM-D638M standard, which was then simplified to a piecewise curve.[10] Finite element analysis of most adhesive joints are generally two-dimensional, often assuming plane strain.[4,7,12,13] It is known that a crack will mainly propagate in plane strain conditions due to the constraint from the adherend of the adhesive joints. The recent work of Richardson *et al.*,[8] comparing two- and three-dimensional finite element analysis, revealed that the adhesive (with a bond thickness of 2 mm) remains in plane strain over most of the specimen thickness. They showed that the two-dimensional FEA provides adequate requirement to evaluate the stress state and the fracture analysis of the adhesive joints. In the present study, a two-dimensional FEM consisting of eight-noded quadrilateral plane strain elements was developed, in which coarse meshes were considered for the adherend and fine meshes were used around the crack tip region for the adhesive material (see Fig. 1a). Singular elements were employed to evaluate the stress state for a sharp crack tip. A finite crack tip radius (R) of 0.01 mm was also used to study the effect of crack-tip blunting and to determine the crack tip opening displacement (CTOD) for different adhesive bond thickness using the large strain theory of plasticity. Figures 1b and 1c show the mesh configurations around sharp and

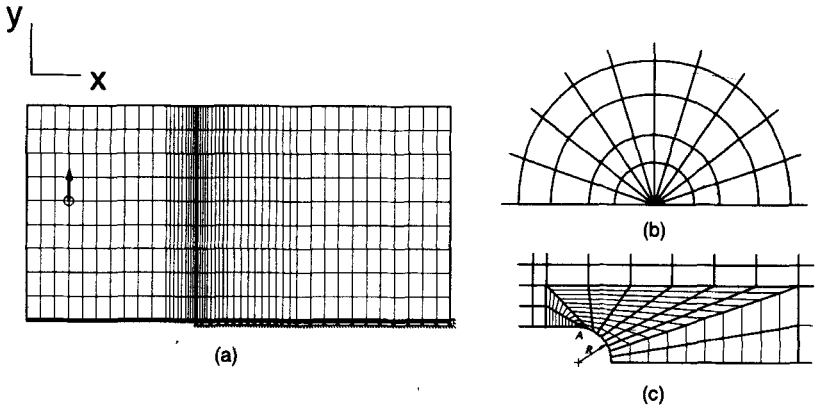

FIGURE 1 (a) Finite element model of CT adhesive joint, (b) mesh configuration around sharp crack tip, (c) mesh configuration around crack tip of finite radius.

finite radius crack tips. The CTOD was determined from the deformed crack opening profile, *i.e.* the vertical displacement of point A in Figure 1c.[14,15] The results revealed that CTOD was independent of R when $0.001\,\text{mm} < R < 0.01\,\text{mm}$. A typical finite element model involved 937 elements with 3016 nodes. The analyses were carried out by both ABAQUS[16] and ADINA[17] software which are widely used to analyse the adhesive joints by other investigators.[18,19]

3 RESULTS AND DISCUSSION

3.1 Stress Distributions Ahead of Crack Tip

Figure 2 shows the distributions of σ_{xx} and σ_{yy} ahead of a sharp crack tip (X denotes the ligament length from the crack tip) for a typical CT adhesive joint for $t = 0.2\,\text{mm}$ subjected to the critical load, P_C. Both σ_{xx} and σ_{yy} represent high stresses within the singular region. Along the ligament length up to about 20 mm from the crack tip, σ_{yy} is

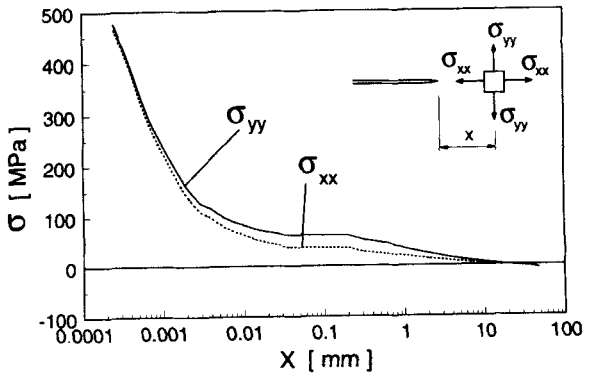

FIGURE 2 Stress distributions ahead of a sharp crack tip ($t = 0.2\,\text{mm}$).

tensile, and then σ_{yy} becomes compressive. Figure 3 shows the distribution of the hydrostatic tensile stress, σ_m, ahead of the crack tip, which has a distribution similar to σ_{yy}.

The effect of adhesive bond thickness on the crack tip stress distributions was evaluated at a constant load (120 N/mm). Figure 4 shows, σ_{yy} normalised by the 0.2% offset yield stress, σ_0, for the bulk adhesive and the joints with different bond thickness, in a log-log plot. From comparisons of various curves of σ_{yy}, the bulk specimen has the highest value. This is attributed to the higher stiffness (Young's modulus) of the adherends than that of the bulk adhesive[5,7] ($E = 71$ GPa and 3.15 GPa, respectively). Also, at $t = 0.05$ mm, σ_{yy} is at least twice as high as at $t = 0.2$ mm at a distance between 0.01 to 0.1 mm ahead of the crack tip. Further increase in the bond thickness from $t = 0.2$ mm to $t = 2$ mm reduces σ_{yy} more. However, σ_{yy} approaches the same value at about 10 mm from the crack tip for both the bulk adhesive and the adhesive joints with different adhesive bond thickness. In the singular domain ($0 < X < 2 \times 10^{-3}$ mm),[5,7] σ_{yy} has a unique slope ($-1/2$) for all t, though the singular region for the bulk adhesive extends to 0.3 mm ahead of the crack tip. For the adhesive joint with $t = 0.05$ mm, σ_{yy} shows a plateau between $X = 0.01$ and 0.1 mm. For larger bond thickness, similar observations can be seen but they occur at a distance further from the crack tip. Figure 5 shows the distributions of σ_{yy} ahead of a finite radius crack tip for both bulk

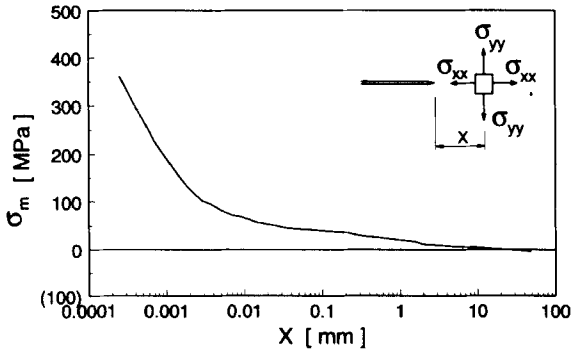

FIGURE 3 Hydrostatic stress (σ_m) distribution ahead of a sharp crack tip ($t = 0.2$ mm).

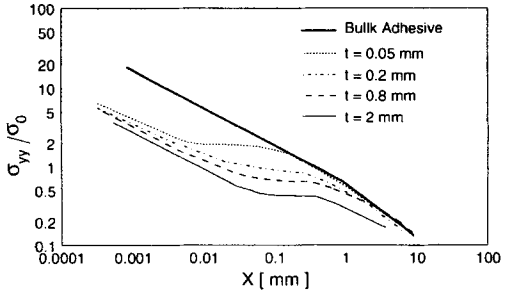

FIGURE 4 σ_{yy} distributions ahead of a sharp crack tip in bulk adhesive and in adhesive joints with different bond thicknesses.

adhesive and adhesive joints with different bond thickness. For adhesive joints, σ_{yy} increases rapidly from the near-crack tip region and approaches a maximum value at a small distance from the crack tip ($X = 1.5 \times 10^{-2}$ mm), though, for the bulk adhesive, σ_{yy} has a maximum at a greater distance. This difference is due to the lower stiffness of the bulk adhesive, which results in a high stress state for a longer distance than that in the adhesive joints. For $X > 0.1$ mm, σ_{yy} has similar characteristics to those for a sharp crack for different bond thickness. Comparison of Figures 4 and 5 shows that the stress state near the sharp crack tip has singular characteristics and a high stress state is present. This is different from the distribution of σ_{yy} for the finite radius crack tip case. These results are consistent with the finite element analysis by McMeeking[14] for an isotropic material with a crack tip of finite radius, where the singular stress state near the crack tip is relieved by intensive deformation around a blunted crack tip.

3.2 Effect of Adherend Stiffness on *J*

The dependence of J on the Young's modulus of the adherend, E_2 (normalised by the adhesive modulus, E_1), for the joints with different bond thickness is given in Figure 6 for an applied load of 100 N/mm. J decreases as the adherend stiffness is increased.

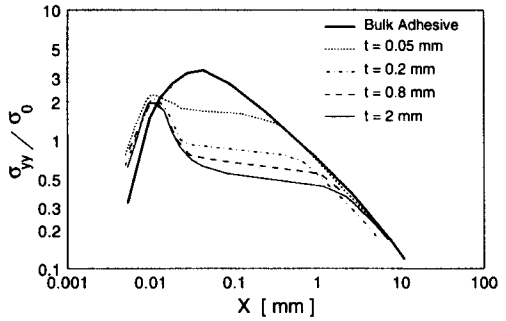

FIGURE 5 σ_{yy} distributions ahead of a finite radius crack tip in bulk adhesive and in adhesive joints with different bond thicknesses.

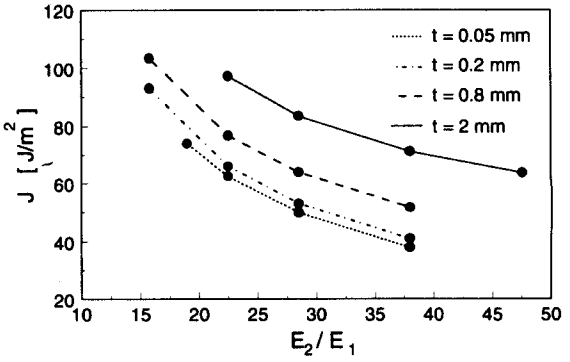

FIGURE 6 J as a function of normalised Young's modulus of adhesive for different bond thicknesses. (Applied load is 100 N/mm).

Wang[5] found that for a DCB adhesive joint specimen with $E_2/E_1 = 20$, σ_{yy} near the crack tip decreased to about one-fifth of that in the bulk adhesive specimen ($E_2/E_1 = 1$). Therefore, as the stiffness of the adherend is reduced, a high stress is produced, so that stress, combined with the ability of the adhesive to accommodate more extensive plastic deformation at the crack tip, resulted in a higher J. The results in Figure 6 confirm this argument.

3.3 Constraint Parameters

3.3.1 J-Q theory and constraint effect

The stress distributions ahead of the crack tip for a power-hardening material can be characterised in terms of the J-integral by Hutchinson,[20] Rice and Rosengren,[21] commonly called the HRR solution. The stress, σ_{ij}, and strain, ε_{ij}, fields are given by:

$$\sigma_{ij} = \sigma_0 \left(\frac{EJ}{\alpha \sigma_0^2 I_n r} \right)^{\frac{1}{n+1}} \sigma_{ij}(\theta, n) \tag{1}$$

$$\varepsilon_{ij} = \frac{\alpha \sigma_0}{E} \left(\frac{EJ}{\alpha \sigma_0^2 I_n r} \right)^{\frac{1}{n+1}} \varepsilon_{ij}(\theta, n) \tag{2}$$

where θ and r are the polar coordinates, E the Young's modulus, α a material constant, n a hardening parameter, σ_0 the yield stress, I_n an integration constant and J is the amplitude of the HRR singularity defined by the path-independent J-integral.[21] The HRR solution is based on the constraint around the crack tip in an infinite plane-strain medium, which results in a high triaxial stress state, a stress state that is too high to be realised for any finite-size specimen of real elastic-plastic material. The results of the finite element analysis[14,15] have shown that the triaxiality near the crack tip of finite-size specimens is clearly lower than that of the HRR solution. O'Dowd and Shih[22,23] have introduced a two-parameter theory, J and Q, to characterise a full range of high and low triaxial stress states near the crack tip, where J sets the size scale of the process zone over which large stresses and strains develop, while Q scales the near-crack-tip stress state relative to a reference stress state (*i.e.* the HRR field) with a high triaxility. The Q field is defined by:

$$\mathbf{Q} = \frac{\sigma_{\theta\theta} - \sigma_{\theta\theta}|_{\mathrm{HRR}}}{\sigma_0} \tag{3}$$

where $\sigma_{\theta\theta}$ is the actual angular stress, $\sigma_{\theta\theta}|_{\mathrm{HRR}}$ the corresponding HRR stress component. This field is defined within the sector $|\theta| < \pi/2$ and $J/\sigma_0 < r < 5J/\sigma_0$. However, for definition, Q is evaluated at $r = 2J/\sigma_0$ and $\theta = 0$.[22,23] In fact, Q is a natural measurement of the stress triaxiality near the crack tip, or the crack tip constraint relative to a reference stress state with a high triaxiality.

In this work, the Ramberg-Osgood power-law idealisation was used to describe the nonlinear and strain-hardening behaviour of the adhesive material in uniaxial tension given by:

$$\varepsilon = \frac{\sigma}{E} \left[1 + \alpha \left(\frac{\sigma}{\sigma_0} \right)^{n-1} \right] \tag{4}$$
$$= \varepsilon_e + \varepsilon_p$$

where ε_e and ε_p are elastic and plastic strains, respectively. Figure 7 shows the logarithmic stress-plastic strain curve of the bulk adhesive material from which n can be determined. Figure 8 shows the distributions of σ_{yy} normalised by σ_0 as a function of the normalised distance, $X\sigma_0/J$, for a sharp crack tip when the fracture loads are applied in FEM for different bond thickness. The difference between the stress state of the HRR field and that in the CT adhesive joints indicates that the degree of triaxiality or crack tip constraint in the joints was much lower than that in the HRR field.[23] Furthermore, for the small adhesive thickness ($t = 0.05$ mm), the stress state is clearly influenced by the constraint of the aluminium adherends and it involves a higher degree of stress triaxiality compared with that in the bulk adhesive. With increasing bond thickness, the constraint is reduced towards that of the bulk adhesive material. The stress triaxiality as characterised by Q is shown in Figure 9 for the adhesive joints with different bond thickness. The considerable difference in the triaxiality between the stress states of the adhesive joints and the HRR field confirms that the high constraint defined by the HRR stress field is effectively relieved for finite size geometries.[24]

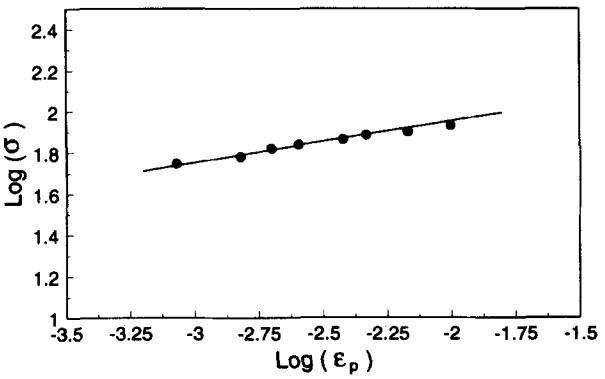

FIGURE 7 Logarithmic stress-strain curve of bulk adhesive material under uniaxial tension.

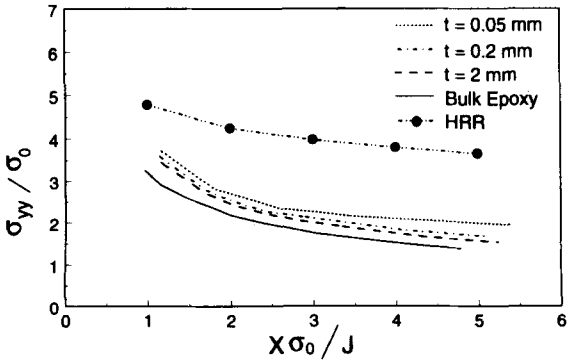

FIGURE 8 HRR stress solution and normalised distributions of σ_{yy} ahead of crack tip in bulk adhesive and in adhesive joints with different t.

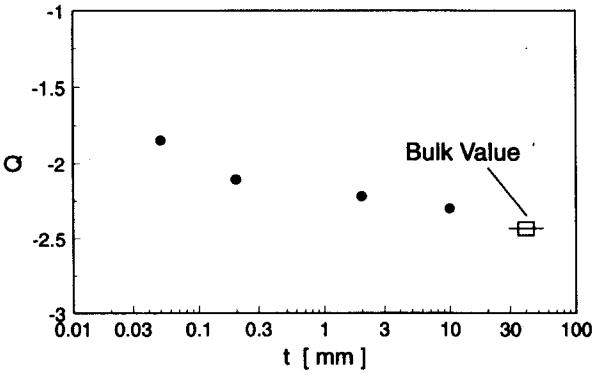

FIGURE 9 Q value as a function of adhesive bond thickness.

3.3.2 *J-CTOD relationship and constraint effect*

For elastic-plastic materials, characteristics of the stress state around the crack tip can be described by either J or CTOD.[25] For a power-hardening material, a unique relationship exists between those two parameters given by:[26]

$$J = m\sigma_0 CTOD \tag{6}$$

where m is a dimensionless constant which is an indication of the constraint and depends on the stress state and material properties. The difference in Q value for the stress states around the crack tip in the adhesive joints indicates that the relationship between J and CTOD might be different for different bond thickness. To evaluate the constraint effect of the adherends on the J-CTOD relationship a crack tip of finite radius is used in the FEA. Both J and CTOD are calculated at different load levels for different bond thickness. A straight line J-CTOD relationship for each bond thickness is established in Figure 10. From the slope of each line and a constant yield stress of the adhesive material (*i.e.* $\sigma_0 = 0.2\%$ offset yield stress), m can be evaluated for different

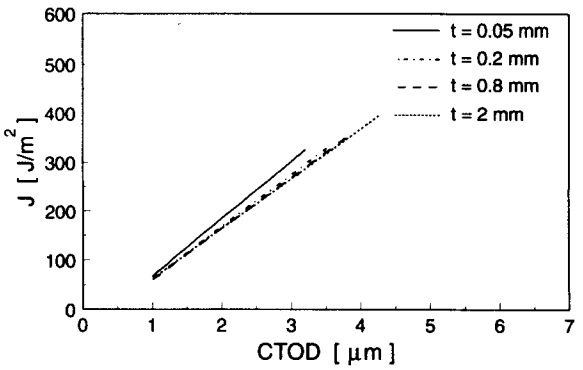

FIGURE 10 Linear relationship between J and CTOD for different bond thickness.

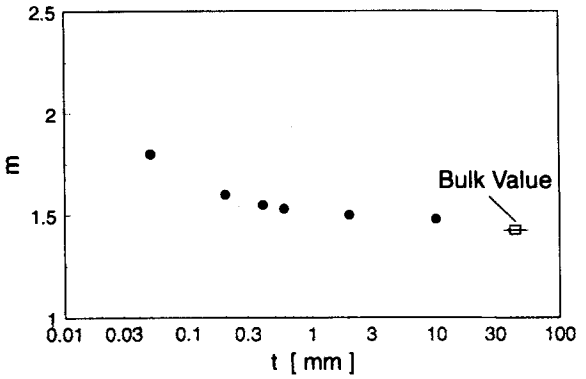

FIGURE 11 Constraint parameter, m, as a function of adhesive bond thickness.

bond thickness. The variation of m as a function of bond thickness, t, is shown in Figure 11. The results indicate that the constraint of the adherend has limited the crack tip plastic deformation for small adhesive bond thickness ($t < 0.2$ mm) and, therefore, high values of m are obtained, while for large bond thickness ($t > 0.2$ mm), m is reduced asymptotically toward the value of the bulk adhesive. A high constraint, therefore, produces a small crack-tip-opening displacement and *vice versa.*

3.3.3 *Relationship between fracture energy and constraint parameters*

It has been argued that the fracture energy in the adhesive joints is directly related to the stress and strain fields around the crack tip. From the results in the previous sections, it can be seen that either parameter Q or m describes the degree of constraint; the higher the value of Q or m, the higher the constraint around the crack tip. Thus, from Figure 9 and 11, the high constraint in the adhesive joints is clearly reduced as the bond thickness is increased. Consequently, extensive deformation and plastic flow would be promoted and the fracture energy would increase toward the value of the bulk adhesive. Therefore, the fracture energy of the adhesive joints is highly dependent on the crack tip constraint. The higher the constraint is, the lower the fracture energy.

4 CONCLUSIONS

An elastic-plastic finite element analysis (FEA) has been conducted to investigate the constraint effect of adherends on the stress states in compact tension (CT) adhesive joints. Finite element models (FEM) were generated for both sharp and finite radius crack tips. The stress states near the crack tip were evaluated for the bulk adhesive and for the adhesive joints with different bond thicknesses. The stress distributions ahead of the crack tip were obtained for both sharp and finite radius crack tips. Based on J-Q theory, the stress triaxiality near the crack tip in the bulk adhesive and adhesive joints with different bond thickness is determined and compared with the HRR stress field. The results confirm that the high triaxiality of the HRR field is relieved by the extensive

deformation field around the crack tip in the CT specimens. There is no unique relationship between the J-integral and the crack-tip-opening displacement (CTOD) for different bond thickness because the constraint is not a constant.

Based on the results of the present work, the following conclusions can be made:

(a) As the bond thickness is increased, the constraint and/or stress triaxiality at the crack tip is reduced.
(b) When the constraint at the crack tip is reduced, the fracture energy of the adhesive joint is significantly increased tending toward that of the bulk adhesive material.
(c) The J-CTOD relationship is dependent on the constraint at the crack tip. At the same level of applied J, a high constraint produces a small crack-tip-opening displacement, which indicates that the plastic deformation of the material around the crack tip is suppressed.

Acknowledgements

The authors wish to thank Dr. S. X. Wu for his assistance in finite element analysis and discussions on the J-Q theory.

References

1. D. L. Hunston and W. D. Bascom, *ACS Advances in Chemistry Series No. 208: Rubber-Modified Thermoset Resins*, C. K. Riew and J. K. Gillham, Eds. (Amer. Chem. Soc., Washington, 1984), pp. 83–99.
2. H. Chai, *7th ASTM Symp. on Composite Materials, Testing and Design*, **ASTM STP 893**, J. M. Whitney, Ed. (Am. Socy. for Testing and Maths., Philadelphia, 1986), pp. 209–231.
3. H. Chai, *Engineering Fracture Mechanics*, **20,** 413 (1986).
4. S. Mall and G. Ramamurthy, *Int. J. Adhesion and Adhesives*, **9,** 33 (1989).
5. S. S. Wang, J. F. Mandell and F. J. McGarry, *J. Fracture*, **14,** 39 (1978).
6. F. Farhad, R. Muki and R. A. Westman, *Int. J. Solids Structures*, **13,** 561 (1977).
7. J. H. Crews, Jr., K. N. Shivakumar and I. S. Raju, *Adhesively Bonded Joints: Testing and Design*, **ASTM STP 981**, W. S. Johnson, Ed. (Au. Socy. for Testing and Maths., Philadelphia, 1988), pp. 119–132.
8. G. Richardson, A. D. Crocombe and P. A. Smith, *Int. J. Adhesion and Adhesives*, **13,** 193 (1993).
9. G. P. Anderson, S. J. Bennett and K. L. Devries, *Analysis and Testing of Adhesive Bonds* (Academic Press, New York, 1977).
10. H. R. Daghyani, L. Ye and Y.-W. Mai, *J. Adhesion*, this issue.
11. H. R. Daghyani, L. Ye, Y.-W. Mai and J. S. Wu, *J. Mater. Sci. Lett.*, **13,** 1330 (1994).
12. W. C. Carpenter and R. Barsoum, *J. Adhesion*, **30,** 1 (1989).
13. D. A. Bigwood and A. D. Crombe, *Int. J. Adhesion and Adhesives*, **9,** 229 (1989).
14. R. M. McMeeking, *J. Mech. Phys. Solids*, **25,** 357 (1977).
15. R. M. McMeeking and D. M. Parks, *Elastic-Plastic Fracture*, **ASTM STP 668,** J. D. Landes, J. A. Begly, and G. A. Clark, Eds. (Am Socy. for Testing and Materials, Philadelphia, 1979), pp. 175–196.
16. Habbit, Karlsson and Sorensen, *ABAQUS User's Manual* (Pawtucket, RI, USA., 1989).
17. ADINA R&D, Inc, U.S.A., 1992.
18. M. Y. M. Chiang and H. Chai, *Int. J. Solids Structures*, **31,** 2477 (1994).
19. Y. Wang and J. G. Williams, *Composite Science and Technology*, **43,** 251 (1992).
20. J. W. Hutchinson, *J. Mech. Phys. Solids*, **16,** 13 (1968).
21. J. R. Rice and G. F. Rosengren, *J. Mech. Phys. Solids*, **16,** 2 (1968).
21. N. P. O'Dowd and C. F. Shih, *J. Mech. Phys. Solids*, **39,** 989 (1991).
23. N. P. O'Dowd, and C. F. Shih, to appear in *ASTM STP for the US 24th National Symposium on Fracture Mechanics* (American Society for Testing and Materials, Philadelphia, 1994).
24. T. L. Anderson, *Int. J. Fracture*, **41,** 79 (1989).
25. C. F. Shih, *J. Mech. Phys. Solids*, **29,** 305 (1981).
26. T. L. Anderson, *Fracture Mechanics, Fundamentals and Applications* (CRC Press, Boca Raton, Ann Arbor, Boston, 1991), p. 156.